Title
The corneas of naive mice contain both CD4+ and CD8+ T cells.

Journal
Molecular vision, 13

ISSN
1090-0535

Authors
Mott, Kevin R
Osorio, Yanira
Brown, Donald J
et al.

Publication Date
2007-09-28

Peer reviewed

Molecular Vision 2007; 13:1802-12 <http://www.molvis.org/molvis/v13/a201/>
Received 8 August 2007 | Accepted 25 September 2007 | Published 28 September 2007

The corneas of naive mice contain both CD4+ and CD8+ T cells

Kevin R. Mott,[1] Yanira Osorio,[1] Donald J. Brown,[2] Naoyuki Morishige,[2] Andrew Wahlert,[2] James V. Jester,[2] Homayon Ghiasi[1]

[1]Center for Neurobiology & Vaccine Development, Ophthalmology Research Laboratories, Cedars-Sinai Medical Center Burns and Allen Research Institute, Los Angeles, CA; [2]The Eye Institute, University of California Irvine, School of Medicine, Irvine, CA

Purpose: To determine if the corneas of naive mice contain resident CD4+ and CD8+ T cells.
Methods: The presence of T cells in the corneas of naive BALB/c, C57BL/6, and SCID mice was determined by immunostaining with anti-CD4 (clone RM4-5) and anti-CD8 (clone 5H10-1) monoclonal antibodies. Immunostained corneal sections were examined by light microscopy, and immunostained intact corneas were examined by confocal microscopy. The levels of CD4 and CD8 mRNA transcripts in the corneas were determined by TaqMan reverse-transcriptase polymerase chain reaction (RT-PCR) analysis and compared with the expression of these transcripts in the corneas of HSV-1 infected mice. Finally, the number of CD4+ and CD8+ T cells in the cornea of BALB/c, C57BL/6, and ICR mice was determined by cell sorting.
Results: Both light microscopic examination of corneal sections and confocal microscopic examination of intact corneas revealed the presence of CD4+ and CD8+ cells in the central and peripheral regions of the corneas of BALB/c and C57BL/6 mice. Stained cells were not detected in corneas of control SCID mice. CD4 and CD8 mRNA transcripts were detected in corneas of BALB/c and C57BL/6 mice while there were markedly lower levels of transcripts in SCID mice. The number of CD4 transcripts was lower than the number of CD8 transcripts in the corneas of both BALB/c and C57BL/6 mice. Finally, cell sorting showed the presence of both CD4+ and CD8+ T cells in corneas of BALB/c, C57BL/6, and ICR mice.
Conclusions: CD4+ and CD8+ T cells are present in corneas of naive C57BL/6, BALB/c, and ICR mice.

The eye is considered an immune privileged site in which the immune privilege is maintained via mechanisms that attenuate both innate and adaptive immune responses [1,2]. This "immunologically privileged status" may reflect evolutionary pressure to down-modulate certain actions of immune cells within the eye in general and the cornea in particular. The cornea is a highly organized group of cells and proteins but, in contrast to most of the tissues in the body, it does not normally contain blood or lymphatic vessels [3]. However, vascularization of the cornea and infiltration with T cells can occur following surgical manipulation or in certain corneal diseases.

It is generally believed that normally, corneas of mice, rats, and humans are devoid of CD4+ and CD8+ T cells. This conclusion is based on the failure to detect these cells by immunostaining or reverse-transcriptase polymerase chain reaction (RT-PCR) techniques [1,4]. CD4 mRNA was not detected in the corneas of patients with pseudophakic bullous keratopathy [5], and neither CD4+ nor CD8+ cells were detectable by immunostaining of control dystrophic opaque human corneas [6]. In sheep, CD4+ and CD8+ T cells were detected in the cornea by immunostaining only after orthotopic penetrating keratoplasty and several days after the onset of graft rejection [7]. In mice, CD4+ and CD8+ cells were not observed after immunostaining of the corneas of C57BL/6, C57BL/10, B10.D2/nSn, BALB/c, BALB/cBy, BALB.B, or BALB.K sham-treated mice [8,9]. Using the same monoclonal antibodies as those used in the above studies, we previously did not detect any T cells in the corneas of uninfected control BALB/c and C57BL/6 mice or in the corneas of HSV-1 infected BALB/c and C57BL/6 mice by day 1 post-infection [10,11].

Although T cells are apparently absent in the corneas of naive mice, they appear rapidly following trauma. For example, we have detected CD4+ T cells but not CD8+ T cells in the cornea of BALB/c mice as early as three days post-infection with HSV-1 [10,11]. We therefore considered the possibility that T cells are present in the cornea of naive mice but are not detectable by immunostaining using the commonly used monoclonal antibodies. Most of the immunostaining studies of the corneas of naive mice have been based on the use of a limited number of monoclonal antibodies, with clone H129.19 and clone GK1.5 being used to detect CD4 and clone 53.6.7 and clone 2.43 being used to detect CD8. It is possible that the epitopes recognized by these monoclonal antibodies are not readily accessible due to the unique structure of the cornea. It is also possible that the apparent absence of T cells in the corneas of naive mice is due to their low frequency. We therefore revisited the issue of the presence or absence of T cells in the corneas of naive mice using an approach in which we immunostained sections of the cornea or the intact corneas with monoclonal antibodies that recognize epitopes that differ from those analyzed previously with comprehensive examination by light microscopy and confocal microscopy. In

Correspondence to: Homayon Ghiasi, Ph.D., Cedars-Sinai Medical Center, Ophthalmology, 8700 Beverly Blvd D2024, Los Angeles, CA 90272; Phone: (910) 423-0593; FAX: (310) 423-0302; email: ghiasih@cshs.org

addition, we confirmed the results of our immunostaining studies through the use of TaqMan RT-PCR and cell sorting.

METHODS

Mice: Inbred female BALB/c, C57BL/6J mice, and BALB/c-SCID mice of six to eight weeks of age, were purchased from the Jackson Laboratory (Bar Harbor, ME) were used in this study while the ICR mice were purchased from Harlan Sprague Dawley (Indianapolis, IN). All mice were pathogen free and were housed in static microisolator cages in negatively pressurized cubicles to minimize the unlikely possibility of contamination. Animals were handled in accordance with the ARVO statement for the Use of Animals in Ophthalmic and Vision Research.

Ocular infection: Female BALB/c or C57BL/6 mice were infected ocularly with an inoculum of $2x10^5$ PFU/eye of HSV-1 strain McKrae in 2 μl of tissue culture medium. The virus inoculum was placed in each eye without anesthesia or corneal scarification.

Preparation of corneal sections for light microscopy: Corneas were removed at necropsy and snap frozen individually in an isopentane-liquid nitrogen bath and stored at -80 °C. Transverse sections (5 μm thick) of the entire cornea were cut, air-dried overnight, and fixed in acetone for 3 min at 25 °C [10]. Consecutive sections from three sets of isolated corneas were immunostained as we have described previously except that in the current study, we used purified anti-mouse CD4 (clone RM4-5) [12,13] and purified anti-mouse CD8 (clone 5H10-1) [14,15], were purchased from Biolegend (San Diego, CA). Briefly, corneal sections were incubated with each antibody for 30 min at 37 °C and then incubated with biotin-conjugated goat anti-rat IgG. This was followed by incubation of the tissue sections with a complex of avidin-biotin horseradish peroxidase for 20 min and then the red chromogen substrate, aminoethylcarbazol (AEC). For each mouse strain, 20 sections from four mice corneas were stained with anti-CD4 or anti-CD8 mAb.

In some experiments, sequential double immunofluorescent staining on corneal sections from BALB/c or control SCID mice was performed. Sections were incubated with rat anti-mouse CD4 (clone RM4-5) or rat anti-mouse CD8 (clone 5H10-1) mAb for 2 h at 25 °C. TRITC-labeled donkey anti-rat IgG was then used as a secondary antibody (1 h incubation). To detect CD3, Armenian hamster anti-mouse CD3 mAb (clone 145-2C11) and FITC-labeled goat anti-Armenian hamster IgG was used as described above. Stained sections were photographed using an Opympus BX40 epifluorescence microscope equipped with a MicroFire color digital camera (Optronics, Goleta, CA). Batches of cross-adsorbed secondary antibodies (Jackson ImmunoResearch Laboratories, Inc., West Grove, PA) were carefully selected to work only against intended species. Routine controls with primary antibody omission were negative.

Immunohistochemistry and confocal microscopy: Four BALB/c, C57BL/6 mice, and three SCID mice were euthanized and the eyes enucleated and placed in 2% paraformaldehyde in phosphate-buffered saline. The eyes were then fixed overnight, and the corneas were removed and dissected into 1.5x1.5 mm blocks taken from the central and peripheral cornea, excluding the limbus. Each tissue block was then washed in PBS and transferred to a buffer containing anti-TCR, Fc receptor γ subunit (US Biological, Swampscott, MA), diluted 1:100 in PBS and 5% goat serum. Tissue blocks from the right eye of each mouse were then stained with Alexa Fluor 488-conjugated anti-CD4 mAb (clone RM4-5, Biolegend) at 1:100 dilution while the left eyes were stained with FITC-conjugated anti-CD8 antibody (clone 5H10-1, Biolegend) at 1:100 dilution. Tissues were stained for 72 h at 4 °C and then counterstained with 14.3 μM DAPI (Molecular Probes, Invitrogen, Carlsbad, CA). Tissues were then rinsed and mounted in 50% glycerol in PBS. Confocal microscopy was performed using a Zeiss LSM 510 META (Jena, Germany) equipped with a femtosecond titanium-sapphire laser (Chameleon, Coherent, CA). Each block was scanned for the presence of FITC or Alexa Fluor 488-stained cells, and three-dimensional data sets were collected from regions showing positive staining. Each three-dimensional data set was then reconstructed to provide maximum intensity projections in the XY and XZ planes.

RNA extraction and cDNA synthesis: Corneas and spleens from naive BALB/c, C57BL/6, and SCID mice were collected and immersed in RNAlater RNA stabilization reagent and stored at -80 °C until processing. The corneas or spleens from each animal were processed for RNA extraction using TRIzol reagent (Invitrogen) and RNeasy column cleanup (Qiagen Inc., Valencia, CA). Briefly, frozen tissue was resuspended in TRIzol and homogenized, followed by an addition of chloroform and subsequent precipitation using isopropanol. The RNA was then treated with DNase I to degrade any contaminating genomic DNA followed by clean-up using a Qiagen RNeasy column as described in the manufacturer's instructions. The RNA yield from all samples was determined by spectroscopy (NanoDrop ND-1000, NanoDrop Technologies, Inc., Wilmington, DE). On average, the RNA yield from cornea and spleen samples was 1.8-3.75 μg and 50-80 μg, respectively. Finally, 500 ng of total RNA was retrotranscribed with random hexamer primers and Murine Leukemia Virus (MuLV) Reverse Transcriptase contained in the High Capacity cDNA Reverse Transcription Kit (Applied Biosystems, Foster City, CA) all in accordance with the manufacturer's directions. All isolated corneas used for RT-PCR and cell sorting described below were free of contamination from other parts of the mouse eye, vitreous fluid, and tears.

TaqMan real-time polymerase chain reaction: Expression levels of the CD4 and CD8 target genes along with the expression of the endogenous control gene, *GAPDH*, were evaluated using commercially available TaqMan Gene Expression Assays (Applied Biosystems) containing optimized primer and probe concentrations. Primer probe sets consisted of two unlabeled PCR primers and the FAM™ dye-labeled TaqMan MGB probe formulated into a single mixture. Additionally, all probes were designed to overlay an intron-exon junction to eliminate signal from any potential genomic DNA contamination. The assays used in this study were as follows: (1) CD4 ABI ASSAY I.D. Mm00442754_m1 - Amplicon Length=72

bp; (2) CD8 (α chain) ABI ASSAY I.D. Mn01182108_m1 - Amplicon Length=67 bp; and (3) GAPDH ABI ASSAY I.D. Mm999999.15_G1 - Amplicon Length=107 bp.

Quantitative real-time PCR was performed using an ABI PRISM 7900HT Sequence Detection System (Applied Biosystems) in 384 well plates, and all reactions were performed in a final volume of 20 µl. Briefly, all mixtures contained 2 µl of cDNA template, 1X TaqMan Universal PCR Master Mix (2X; Applied Biosystems), and 1X Taqman Gene Expression Assay (CD4, CD8, or GAPDH). Universal thermal cycling conditions were as follows: after an initial 2-min hold at 50 °C to allow AmpErase-UNG activity and 10 min at 95 °C, the samples were cycled 40 times at 95 °C for 15 s and 60 °C for 1 min. Relative gene expression levels were normalized to the expression of the housekeeping gene *GAPDH* (endogenous control) and calculated using the comparative C_T method ($\delta\delta C_T$), described in User Bulletin number 2 provided with the ABI PRISM 7900HT. The $\delta\delta C_T$ method utilizes the assumption that the efficiency of the target amplification and the efficiency of the endogenous control amplification are similar. Therefore, before using this method, efficiencies were evaluated by generating cDNA dilution curves for each primer set. Plots of Ct values versus log cDNA concentrations were constructed and the slopes were calculated using linear regression. The primer efficiency was determined by the formula Efficiency=$10^{(-1/slope)}$ - 1. The calculated primer set efficiencies for CD4, CD8, and GAPDH were 0.98, 0.98, and 0.95, respectively, indicating that the $\delta\delta C_T$ method was valid. Therefore, for a given tissue sample for each animal in the group, real-time PCR was performed in triplicate on the 7900HT System. The threshold cycle (C_T) values, which represents the PCR cycle at which there is a noticeable increase in the reporter fluorescence above baseline, were obtained using SDS 2.2 Software.

In each experiment, an estimated relative copy number for each target gene was calculated using standard curves generated from plasmids containing the gene of interest: pORF-9-mCD8a (InvivoGen, San Diego, CA) and pCMV-Sport1-CD4 (Open Biosystems, Huntsville, AL). Briefly, each plasmid DNA template was serially diluted by 10 fold to contain from 10^3 to 10^{11} copies of the desired gene in 5 µl and was subjected to TaqMan PCR with the same set of primers as test samples. By comparing the normalized threshold cycle of each sample to the threshold cycle of the standards, the copy number for each reaction was estimated.

Isolation of CD4⁺ and CD8⁺ T cells for cell sorting: The corneas from 22-40 mice per strain were isolated free of other parts of the eye and washed in PBS to remove vitreous fluid and tears. The corneas were cut into small pieces and then treated with 3 mg/mL of collagenase type I (Sigma, St. Louis, MO) for 2.5 h at 37 °C, with gentle passage three to four times through an 18 gauge syringe after the first h. The single cell suspensions of total corneal cells were washed three times with PBS and counted. Single cell suspensions of corneal cells were stained with anti-CD4-PE (clone L3T4) and anti-CD8α-PE (clone 53-6.7). During analysis, debris and 7-ADD⁺ cells were excluded through gating. The 7-ADD/CD4/CD8-stained single cell suspensions of corneas were sorted using a MoFlo (Dako North America, Inc., Carpinteria, CA), and the numbers of CD4+7-ADD⁻ and CD8+7-ADD⁻ cells were counted.

RESULTS

Detection of T cells by light microscopic examination of immunostained corneal sections: Three separate batches of three eight-week-old BALB/c and C57BL/6 mice were used to examine the presence of CD4⁺ and CD8⁺T cells in sections of the corneas from naive mice by immunohistochemical analysis. SCID mice, which lack functional T cells, were used as a negative control. Representative photomicrographs of immunostained sections of the corneas from BALB/c, C57BL/6, and SCID mice are provided in Figure 1. No CD4⁺ (Figure 1; SCID CD4⁺) or CD8⁺ (Figure 1; SCID CD8⁺) cells were found in corneal sections from SCID mice. In contrast, CD4⁺ and CD8⁺ T cells were detected in both the stroma (Figure 1; BALB/c CD4⁺ and BALB/c CD8⁺; arrows) and the epithelium (Figure 1; BALB/c CD4⁺ and BALB/c CD8⁺ insets; arrows) from naive BALB/c mice. Similarly, both CD4⁺ and CD8⁺ T cells were detected in stroma (Figure 1; C57BL/6 CD4⁺ and C57BL/6 CD8⁺; arrows) and epithelium (Figure 1; C57BL/6 CD4⁺ and C57BL/6 CD8⁺ insets; arrows) of naive C57BL/6 mice.

The immunostaining procedure described above for CD4⁺ and CD8⁺ T cells suggested that the corneas of naive mice contained both CD4⁺ and CD8⁺ T cell populations. However, all CD4⁺ or CD8⁺ cells are not T cells. Therefore, to show that CD4⁺ or CD8⁺ cells are T cells, corneal sections of naive mice were probed with anti-CD4 and anti-CD3 or with anti-CD8 and anti-CD3 mAbs in double-label experiments as described in Methods. Representative photomicrographs of immunostained sections of the corneas from BALB/c mice are shown in Figure 2. Similar to the single marker immunostaining for CD4⁺ or CD8⁺ T cells, sections of the corneas from BALB/c mice reacted strongly with anti-CD4 antibody (Figure 2; Upper left panel: CD4, red stained cells). The same cells were also positive for CD3 (Figure 2; Upper middle panel: CD3, green stained cells). The merging of these two panels revealed that CD4⁺ T cells were also CD3⁺ (Figure 2; Upper right panel: CD4+CD3 merge, yellow stained cells). Similarly, adjacent sections of the cornea from BALB/c mice reacted strongly with anti-CD8 (Figure 2; Lower left panel: CD8, red stained cells) and anti-CD3 mAb (Figure 2; Lower middle panel: CD3, green stained cells). Merging of these two panels revealed that CD8⁺ T cells were also CD3⁺ (Figure 2; Lower right panel: CD8+CD3 merge, yellow stained cells). As expected, no CD4⁺, CD8⁺, or CD3⁺ T cells were found in corneal sections from SCID mice (data not shown). The observed immunofluorescent staining was judged to be specific based on the following criteria: (1) all secondary antibodies that had cross-adsorbed against several species had been checked in separate experiments using spleen tissue for lack of unwanted interspecies cross-reactivity; (2) double immunostaining of spleen sections (positive control) with the used antibodies revealed specific patterns for each antigen, fully consistent with their expression on spleen cells; (3) omis-

sion of primary antibodies produced a negative staining pattern; and (4) as expected, no $CD4^+$, $CD8^+$, or $CD3^+$ T cells were found in corneal sections from SCID mice (data not shown). Together these results suggest that the $CD4^+$ and $CD8^+$ cells detected in corneas of naive mice are T cells.

Detection of T cells in the cornea by confocal microscopy: Confocal microscopic analysis of corneas that were stained in their entirety revealed the presence of isolated, single cells that were stained with anti-CD4 mAb in two out of the four corneas obtained from BALB/c mice. These were present

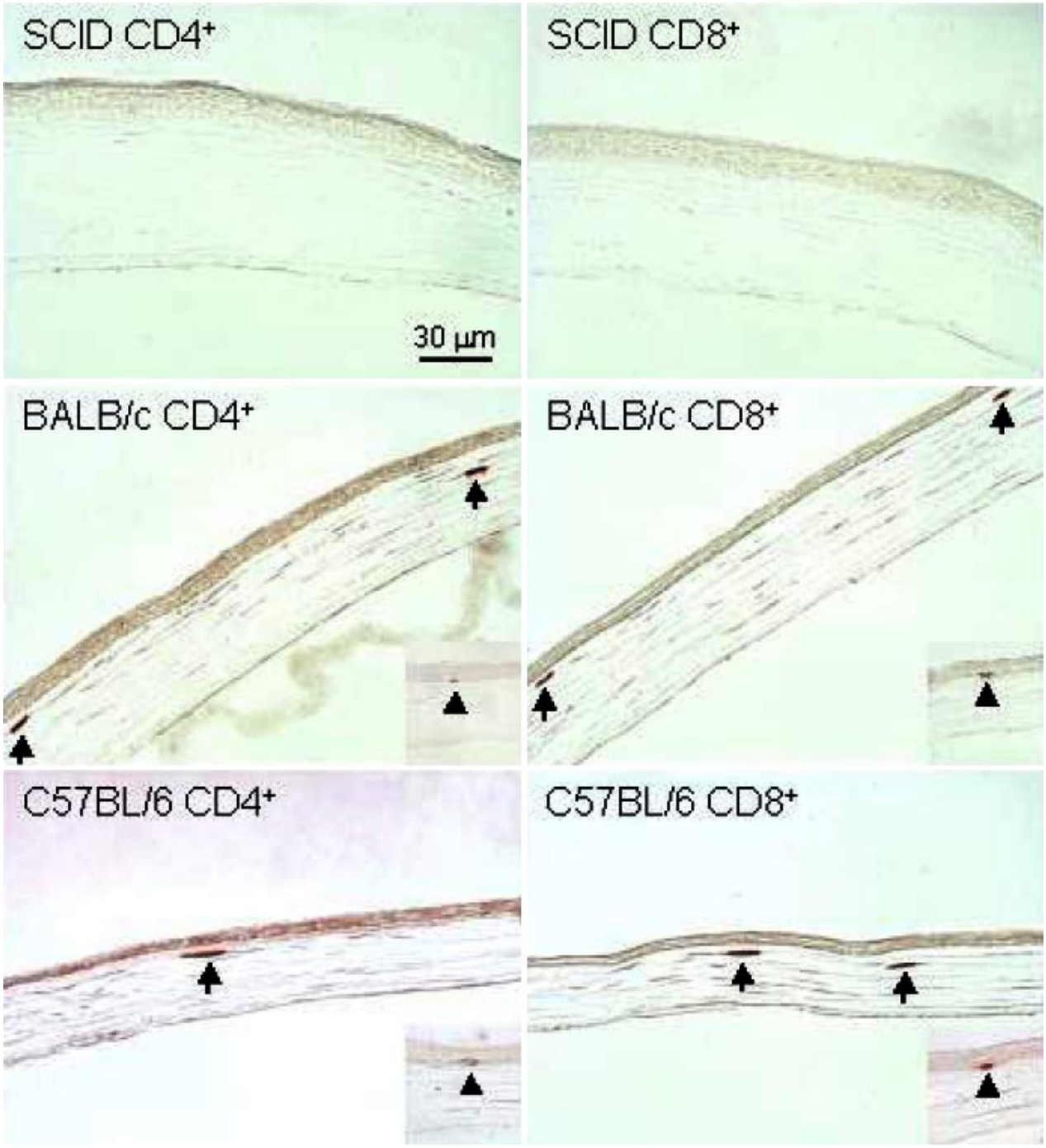

Figure 1. Detection of $CD4^+$ and $CD8^+$ T cells in immuostained sections of the cornea of naive mice by light microscopy. Representative corneal sections from female, eight-week-old naive BALB/c, C57BL/6, and SCID mice stained with anti-CD4 and anti-CD8 antibodies as described in Methods are shown. Panels: Sections of cornea from naive SCID mice were stained with anti-CD4 (SCID $CD4^+$) or anti-CD8 antibody (SCID $CD8^+$). No $CD4^+$ or $CD8^+$ T cells were observed in any of the examined sections. Sections of cornea from naive BALB/c mice were stained with anti-CD4 (BALB/c $CD4^+$) or anti-CD8 antibody (BALB/c $CD4^+$). The arrows show $CD4^+$ and $CD8^+$ T cells in the stroma and epithelial cell layers (insets) of the cornea. Sections of cornea from naive C57BL/6 mice were stained with anti-$CD4^+$ (C57BL/6 $CD4^+$) or anti-$CD8^+$ antibody (C57BL/6 $CD8^+$). The arrows show $CD4^+$ and $CD8^+$ T cells in the stroma and epithelial cell layers (insets) of the cornea.

in both the central and peripheral regions of the cornea (Figure 3A). Using this technique, no anti-CD8-stained cells were detected in the central or peripheral regions of the corneas obtained from the BALB/c mice (Figure 3B). In the C57BL/6 mice, isolated, single cells that were stained with the anti-CD4 monoclonal antibody were observed in two of the four corneas examined. These cells were present in both the central and peripheral regions of the cornea (Figure 3C). In one out of the four corneas from the C57BL/6 mice, $CD8^+$ cells were detected in the central region of the cornea, and in three of four corneas, $CD8^+$ cells were detected in the peripheral region of the cornea (Figure 3D). Neither $CD4^+$ cells (Figure 3E) nor $CD8^+$ cells (Figure 3F) were observed in the corneas of any of the SCID mice.

Detection of CD4 and CD8 transcripts in corneas of naive mice: Corneas and spleens were removed from naive mice and the total RNA was isolated as described in Methods. TaqMan RT-PCR was performed on the total RNA from individual mouse corneas to detect the presence of CD4 and CD8 mRNA. Analysis of levels of CD4 and CD8 mRNA in the spleen of each group was used as a control, and the levels of GAPDH were used as an internal control.

A CD8-specific band of 67-bp was detected in corneas of C57BL/6 and BALB/c mice as well as SCID mice (Figure 4; upper right panel). A similar band was also detected in the spleens (Figure 4; upper left panel). Similarly, a CD4-specific band of 72-bp was detected in the corneas of C57BL/6, BALB/c, and SCID mice (Figure 4; middle right panel). The presence of CD4 mRNA in the spleens of C57BL/6, BALB/c, and SCID mice are shown as a control (Figure 4; middle left panel). Finally, we detected a GAPDH-specific band of 107-bp in all groups (Figure 4; lower panels). The RT controls with no RNA template were negative for all groups (Figure 4; RT control). Thus, these results suggest that corneas of C57BL/6, BALB/c, and SCID mice contain both CD4 and CD8 mRNA.

Our TaqMan RT-PCR results as described above and shown in Figure 4 suggested that CD4 and CD8 mRNA transcripts are present in the corneas of C57BL/6, BALB/c, and SCID mice. We therefore subjected mRNA, isolated from four mice per group, to RT-PCR to determine the expression of CD4 and CD8 mRNA transcripts in the corneas and spleens of C57BL/6 and BALB/c mice compared to the expression in SCID mice. Our results (Table 1) indicated that the levels of CD4 transcripts were higher in the corneas of naive C57BL/6 and the BALB/c mice than in the corneas of naive SCID mice, but the levels of these transcripts in the C57BL/6 mice were much higher (approximately 21 times higher than in SCID mice) than in the BALB/c mice (6.5 times higher than the SCID mice; Table 1). In contrast, although the levels of the CD8 transcripts were higher in the corneas of the naive C57BL/

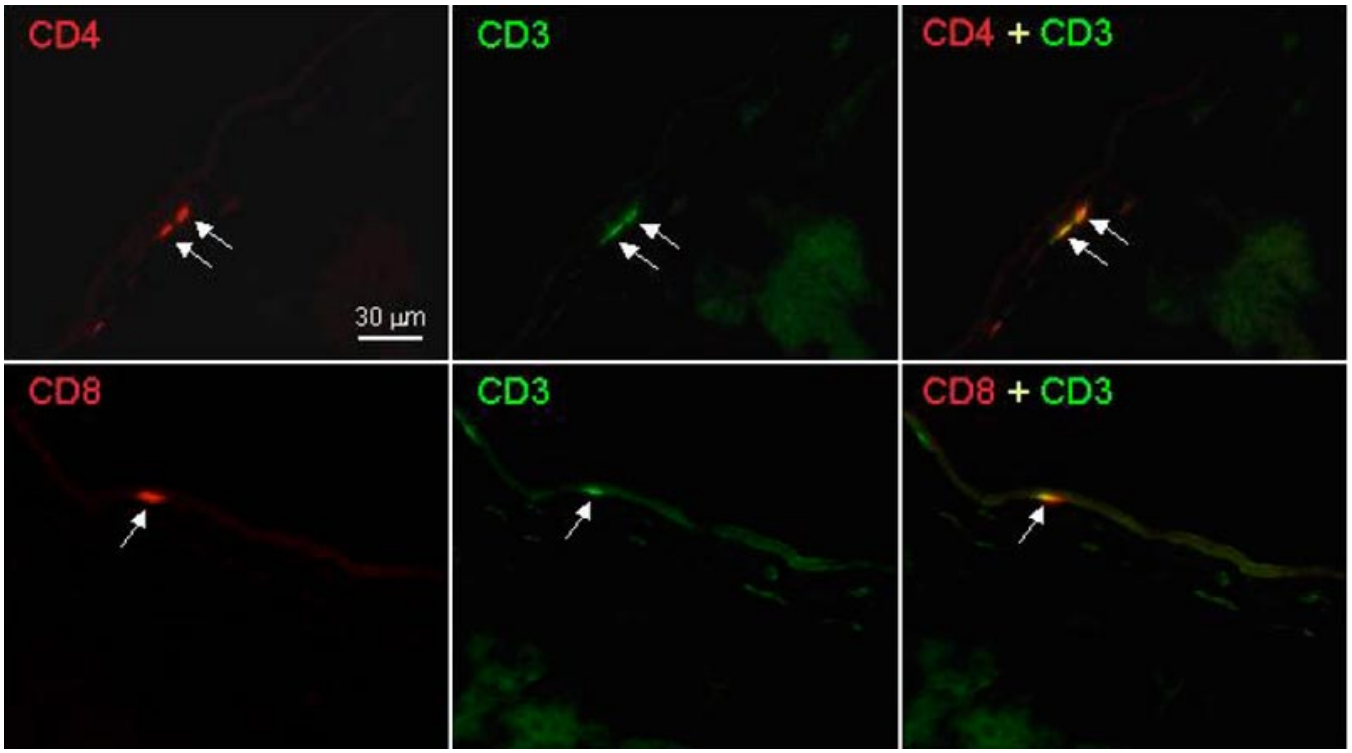

Figure 2. Detection of CD4/CD3-postitive and CD8/CD3-positive T cells in immunostained sections of the cornea of naive mice. Representative corneal sections from naive BALB/c mice stained with anti-CD4 and anti-CD3 or anti-CD8 and anti-CD3 mAbs as described in Methods are shown. Panels: Sections of cornea from naive BALB/c mice were stained with anti-CD4 (CD4), anti-CD3 (CD3), or merged (CD4+CD3). Arrows show $CD4^+$, $CD3^+$, and CD4/CD3 double-positive T cells in the stromal cell layer of the cornea. Sections of the cornea from naive BALB/c mice were stained with anti-CD8 (CD8), anti-CD3 (CD3), or merged (CD8/CD3). The arrows show $CD8^+$, $CD3^+$, and CD8/CD3 double-positive T cells in the stromal cell layer of the cornea.

6 and BALB/c mice than in the corneas of naive SCID mice, the transcript levels were lower than those observed for CD4 transcripts and of a similar magnitude (approximately 3.3 times higher and 2.2 times higher, respectively, as compared with SCID mice; Table 1). Thus, our results indicated that the levels of CD4 and CD8 transcripts were higher in the corneas and spleens of naive C57BL/6 and the BALB/c mice than in the corneas of naive SCID mice.

CD4 and CD8 transcripts in the corneas of BALB/c and C57BL/6 mice: Our TaqMan RT-PCR results as described above and shown in Figure 4 and Table 1 suggested that CD4 and CD8 transcripts were present in the corneas of C57BL/6, BALB/c, and SCID mice. To determine the copy numbers of CD4 and CD8 transcripts, mRNA isolated from eight BALB/c or C57BL/6 mice per group was subjected to RT-PCR. As a positive control, BALB/c or C57BL/6 mice were infected ocularly with HSV-1 strain McKrae, and the copy numbers of CD4 and CD8 transcripts were determined from five mice on the fifth day of post-infection. Approximately 2500-3000 copies of CD4 transcripts per μg of total RNA isolated from cornea of naive BALB/c or C57BL/6 mice were detected (Figure 5A). Copy numbers in the corneas of naive mice were similar to those of the corresponding infected mice (Figure 5A). The differences between the numbers of CD4 transcripts in the corneas of naive versus infected mice were not statistically significant.

CD8 transcripts were also detected in corneas of both BALB/c and C57BL/6 naive mice (Figure 5B). The number of CD8 transcripts in the corneas of BALB/c and C57BL/6 mice was similar and was approximately four times higher than that of the corresponding number of CD4 transcripts (Figure 5A,B). In contrast to the similar level of CD4 transcripts in corneas of both naive and infected mice, the level of CD8 transcripts in the corneas of infected mice was approximately

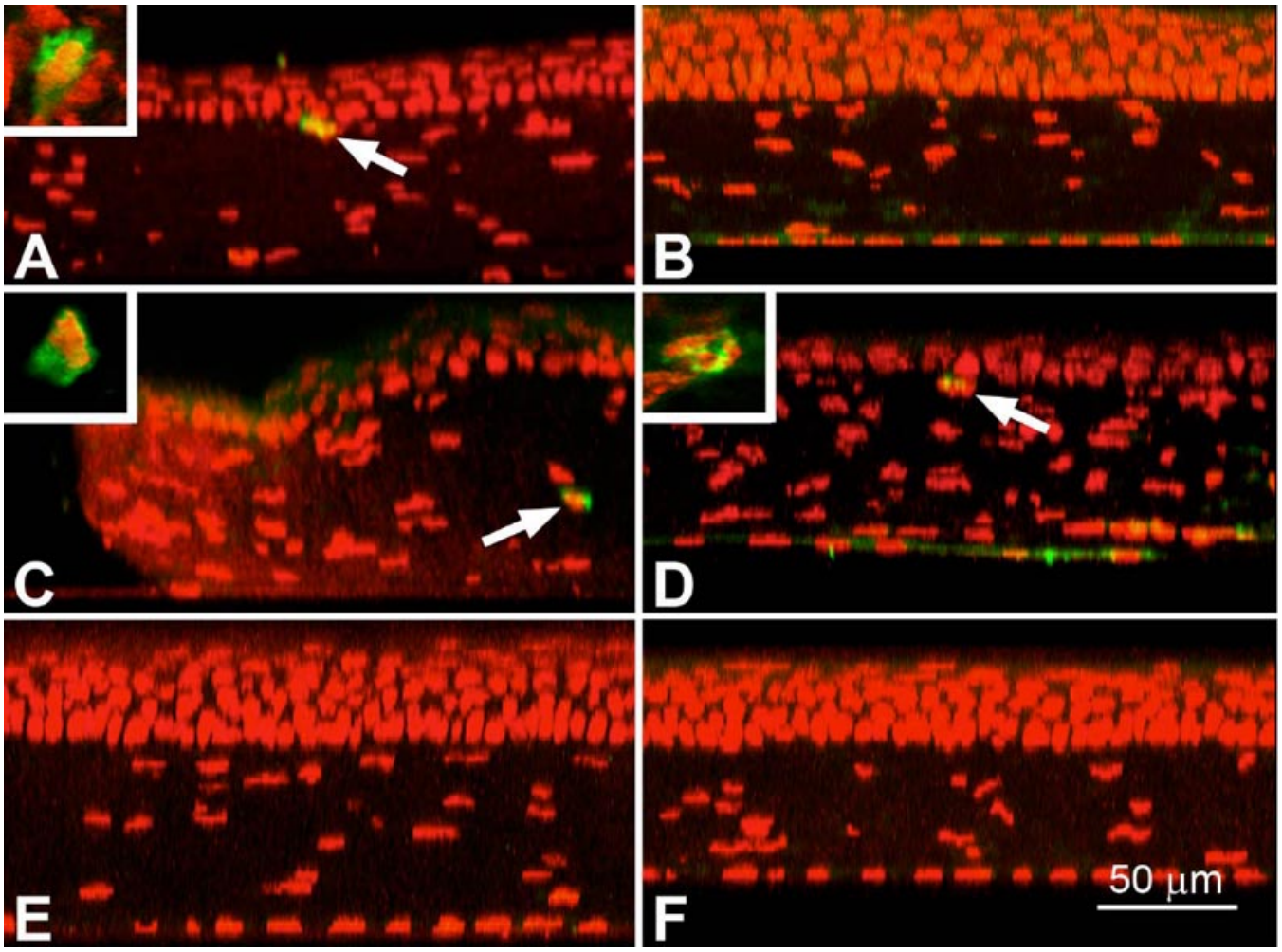

Figure 3. Detection of $CD4^+$ and $CD8^+$ T cells in the intact corneas of naive mice by confocal microscopy. Eight-week-old, female, naive BALB/c, C57BL/6, and SCID mice were euthanized, and their eyes were immersed in 2% paraformaldehyde as described Methods. Cross-sectional projections of BALB/c (**A** and **B**), C57BL/6 (**C** and **D**), and SCID (**E** and **F**) mouse corneas stained with Alexa Fluor 488-conjugated anti-CD4 (**A**, **C**, and **E**) or FITC-conjugated anti-CD8 (**B**, **D** and **F**) monoclonal antibodies are shown. Positive staining appears green. Inserts (**A**, **C** and **D**) show positively stained cells as they appeared in individual optical planes (insert zoomed 2x from projection magnification). Tissue was counter-stained with DAPI to indicate cell nuclei (pseudocolored in red).

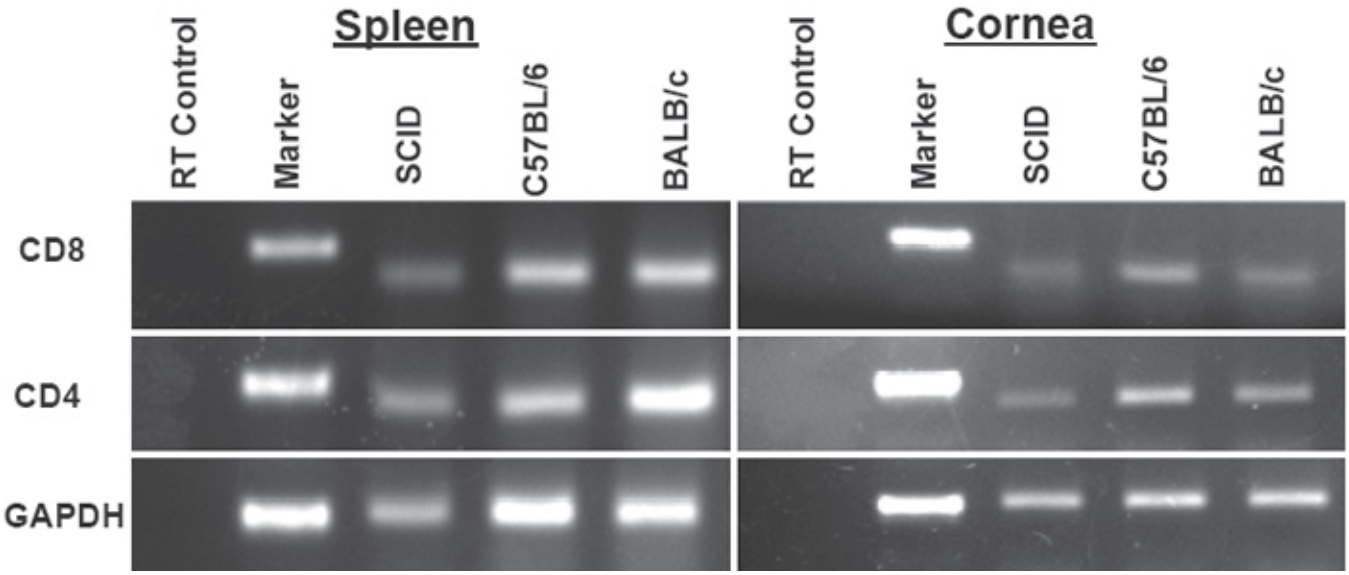

Figure 4. Presence of CD4 and CD8 mRNA in the corneas of naive mice. Corneas or spleens from eight BALB/c or C57BL/6 mice and four SCID mice were harvested. Total RNA was isolated and TaqMan RT-PCR was performed as described in Methods using CD4 and CD8 primers. Following cDNA synthesis, 10 µl of cDNA for each group was run on individual lanes of a 0.9% agarose. The data shown are representative of one of four experiments.

Table 1. Relative quantitation of CD4 and CD8 mRNA transcript expression in cornea and spleen using the comparative C_T method

RNA Source	CD4 C_T	CD8 C_T	GAPDH C_T	ΔC_T CD4 - GAPDH	ΔC_T CD8- GAPDH	$\Delta\Delta C_{T\text{-}CD4}$ ΔC_T-ΔC_T	$\Delta\Delta C_{T\text{-}CD8}$ ΔC_T-ΔC_T	CD4 Relative to SCID	CD8 Relative to SCID
BALB/c Cornea	30.27±1.10	30.91±0.83	18.10±0.89	12.17±1.41	12.80±1.22	-2.70±1.41	-1.11±1.22	6.50 (2.44-17.27)	2.16 (0.93-5.03)
C57BL/6 Cornea	27.97±1.04	29.67±1.30	17.48±1.10	10.50±1.51	12.20±1.70	-4.37±1.51	-1.71±1.70	20.67 (7.26-58.89)	3.27 (1.01-10.63)
SCID Cornea	33.32±1.38	32.36±0.54	18.45±1.21	14.87±1.83	13.91±1.33	0.00±1.83	0.00±1.33	1.00 (0.28-3.55)	1.00 (0.40-2.51)
BALB/c Spleen	23.08±1.18	23.87±1.90	18.58±1.80	4.50±2.21	5.30±2.67	-6.92±2.21	-4.75±2.67	121.10 (26.17-560.27)	26.90 (4.23-171.25)
C57BL/6 Spleen	24.51±1.28	24.91±1.98	19.30±1.86	5.21±2.26	5.61±2.72	-6.21±2.26	-4.44±2.72	74.03 (15.45-354.58)	21.70 (3.29-143.01)
SCID Spleen	29.35±1.70	27.98±0.56	17.93±0.70	11.42±1.84	10.05±0.90	0.00±1.84	0.00±0.90	1.00 (0.28-3.58)	1.00 (0.53-1.87)

A: Quantitative RT-PCR was performed in triplicate using 2 µl of cDNA reverse transcribed from 500 µg of total RNA from individual cornea or spleen samples (four mice for BALB/c and C57BL/6 groups and two mice for SCID group). The mean threshold cycle (C_T) value for each target (CD4 and CD8) and endogenous reference (GAPDH), representing the PCR cycle at which the ABI 7900 HT Detection System first detects a noticeable increase in reporter florescence above baseline signal, was calculated for each group. **B**: The δC_T values for each target were determined by subtracting the mean GAPDH C_T value from the mean CD4 and CD8 C_T values. The standard deviation of the difference was calculated from the standard deviations of the CD4, CD8, and GAPDH values by the formula (s= the square root of $s_1^2 + s_2^2$). **C**: In this study the SCID animal group was chosen as the arbitrary constant and all expression levels are presented as relative to the SCID group. The calculation of $\delta\delta C_T$ involved subtraction of the δC_T of the SCID sample from the δC_T of the compared BALB/c and C57BL/6 samples. The standard deviation is equivalent to the standard deviation of the δC_T. **D**: The range of CD4 and CD8 fold expression relative to the SCID cornea and spleen was determined by the expression: $2\text{-}\delta\delta C_T \pm$ the standard deviation as shown in Figure 4.

five times higher and 3.5 times higher than that of naive BALB/c and C57BL/6 mice, respectively (Figure 5B). As a control, we measured the number of CD4 and CD8 transcripts in the spleens of naive BALB/c and C57BL/6 mice (Figure 5C). While the ratio of CD4:CD8 transcripts in the corneas of naive mice was approximately 1:4, this ratio was 1.2:1 to 1.4:1 in the spleens of BALB/c and C57BL/6 mice (Figure 5). Finally, the numbers of CD4 and CD8 mRNA per μg of total RNA from T cells in corneas of both groups of mice was approximately 1,200 fold and 300 fold lower than that of the corresponding spleens, respectively (Figure 5)

These results suggest that naive BALB/c and C57BL/6 mice have both CD4 and CD8 transcripts in their corneas. Since the level of CD4 transcripts in corneas of infected mice were similar to that of naive mice, our results also suggest no additional $CD4^+$ T cells were detected in the corneas of infected mice on day five post-infection. In contrast, we detected a significant increase in the number CD8 transcripts in the corneas of infected mice compared with naive mice, suggesting that there is activation and/or increase in the flow of $CD8^+$ T cells into the corneas of infected mice by day five post-infection.

Sorting of T cells from cornea of mice: Our results suggest that T cells from the corneas of normal mice contain both CD4 and CD8 transcripts. The discrepancies between our results and previously published data could be due to inaccessibility of CD4 and CD8 T cell epitopes to some of the mAbs that have been used in studies of normal corneas or, alternatively, to lower numbers of $CD4^+$ and $CD8^+$ T cells in normal corneas. To address these possibilities, normal BALB/c, C57BL/6, or ICR mice were sacrificed and corneal cells from 22-40 mice from two separate experiments per strain were isolated by collagenase treatment as described in Methods. $CD4^+$ and $CD8^+$ T cells in the cornea were stained with different mAbs than the ones we used in the above experiments for confocal and light microscopy. The total number of cells and the number of $CD4^+$ and $CD8^+$ T cells per cornea of each group of mice are shown in Table 2. Our cell sorting results showed the presence of both $CD4^+$ and $CD8^+$ T cells in the corneas of BALB/c, C57BL/6, and ICR mice (Table 2). The age of the mice had a significant effect on the number of T cells present in the corneas. Nineteen-month-old ICR mice had a higher number of $CD4^+$ and of $CD8^+$ T cells per cornea than four-week-old ICR mice (Table 2). In both BALB/c and C57BL/6 mice, the number of $CD8^+$ T cells per cornea was similar whereas the number of $CD4^+$ T cells per cornea of BALB/c mice was higher than in C57BL/6 mice (Table 2). These results suggest that both $CD4^+$ and $CD8^+$ T cells are present in low numbers in corneas of normal mice and are detectable with mAbs that did not detect these cells in corneas of normal mice by immunostaining.

Previously, we detected the presence of $CD4^+$ T cell infiltrates in corneas of ocularly infected HSV-1 mice as early as day three post-infection using antibody clone H129.19 and clone GK1.5. In contrast, we did not detect $CD8^+$ T cell infiltrates on days 1, 3, 7, 10, 14, and 21 post-infection using antibody clone 53.6.7 and clone 2.43 [10,11]. Similarly, no other studies reported $CD8^+$ T cell infiltrates in corneas of HSV-1 infected mice during the period of acute viral infection using the above antibodies. However, our TaqMan RT-PCR data shown in Figure 4 suggest that both $CD4^+$ and $CD8^+$ transcripts are present in corneas of naive BALB/c mice. In addition, our cell sorting data demonstrate that the above antibodies can recognize collagenase-digested corneal T cells. Thus, to determine if similar trends are applicable to the presence of $CD4^+$ or $CD8^+$ T cells in corneas of naive mice versus HSV-1 in-

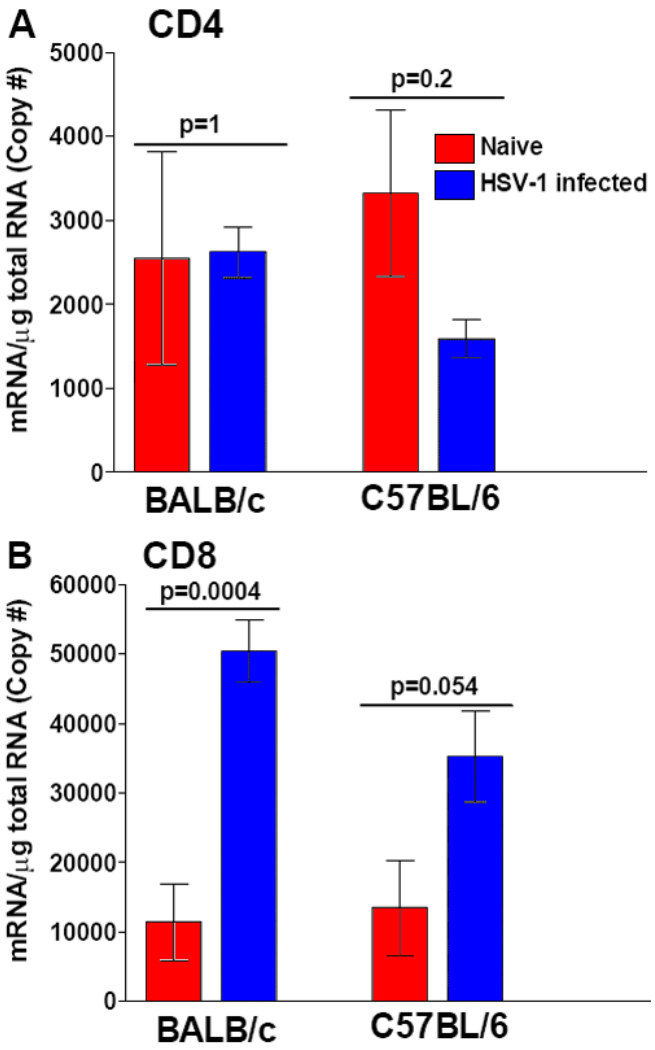

Figure 5. Copy number of CD4 and CD8 transcripts in corneas of naive mice. Corneas and spleens from individual naive BALB/c and C57BL/6 mouse were isolated as described in the legend to Figure 3. TaqMan RT-PCR was performed on total RNA and GAPDH expression was used to estimate the relative expression of CD4 and CD8 mRNA in each individual mouse corneas. As positive control BALB/c and C57BL/6 mice were ocularly infected with $2x10^5$ PFU/eye of highly neurovirulent HSV-1 strain McKrae. Infected mice were euthanized on day 5 post-infection, the corneas of each individual mouse were isolated, and TaqMan RT-PCR was performed on total RNA as above. Each point represents mean±SEM from eight and five mice for naive and infected mice, respectively. Panels: **A** CD4 copy number in cornea; **B** CD8 copy number in cornea; and **C** CD4 and CD8 copy number in spleen.

fected mice, eight-week-old female BALB/c mice were infected ocularly with $2x10^5$ PFU/eye of HSV-1 strain McKrae. Ten mice were used as naive controls. From day 1 to day 5 post-infection, ten mice per time point were euthanized, their corneas were isolated and used for cell sorting. The data show that both $CD4^+$ and $CD8^+$ T cells are present in corneas of infected mice (Figure 6). The number of T cells in corneas of infected mice compared with naive mice increased from day one to day two for $CD4^+$ T cells while the number of $CD8^+$ T cells increased from day one to day three post-infection (Figure 6). There was a sharp decline in the number of both subpopulations of T cells thereafter. These results confirm our two main hypotheses that both $CD4^+$ and $CD8^+$ T cells can be detected in corneas of normal mice following collagenase treatment, but they are present in low numbers.

DISCUSSION

The cornea is a simple solid organ that is comprised of epithelial cells, keratocytes, and endothelial cells in three distinct layers [1]. Blood and lymph vessels are absent from the normal central cornea [16]. It was previously thought that the cornea was devoid of bone marrow-derived cells except for the rare Langerhans' cells in the epithelium near the limbus [17,18]. However, recent data suggest that 5%-10% of corneal stromal cells are derived from the bone marrow [19,20]. At the same time, it has been reported that normal rodent and human corneas lack detectable levels of $CD4^+$ and $CD8^+$ T cells as determined by RT-PCR or immunostaining [1,4-6,8-11]. The absence of $CD4^+$ and $CD8^+$ T cells in healthy cornea was suggested to be due to T cell death by apoptosis [21]. In our current study, we used a different set of monoclonal antibodies than those used in the previous works, a more thorough analysis of the entire cornea to detect cells present in low frequency, and a more sensitive analysis of mRNA. Our results indicate that both $CD4^+$ and $CD8^+$ T cells are present in low numbers in the corneas of naive mice.

Immunostaining of sectioned corneas of naive mice revealed the presence of CD4/CD3-postive and CD8/CD3-positive cells in both the central and peripheral regions of all of the corneas examined. Confocal microscopic analysis of intact, stained corneas also revealed the presence of $CD4^+$ and $CD8^+$ T cells in the corneas of some but not all of the C57BL/6 mice. $CD4^+$ T cells were observed in the corneas of some of the BALB/c mice, but $CD8^+$ T cells were not detected in the corneas of any of the BALB/c mice when they were examined by confocal microscopy. This discrepancy between the results obtained using light microscopy examination of stained sections and confocal microscopy examination of the stained intact corneas may indicate that the staining is limited by the accessibility of the antibody to the cells. Alternatively, it may simply reflect the relative sparcity of the T cells. Similarly, the discrepancy between the results of our current studies and the previously published studies may reflect the use of different antibodies or the relatively sparse numbers of $CD4^+$ and $CD8^+$ T cells. Finally, it would be of interest to determine if functional CD4/CD3-positive and CD8/CD3-positive T cells are present in normal and SCID mice corneas. However, these studies would be prohibitive due to the need of a large number of mice and an excessive cost to carry out these analyses since there are only few of these cells per cornea.

The presence of CD4 and CD8 transcripts in the corneas of naive C57BL/6 and BALB/c mice confirmed the presence of cells expressing these markers as determined by microscopic examination of immunostained tissues and cell sorting. The copy numbers of CD4 and CD8 transcripts in corneas of both BALB/c and C57BL/6 mice were approximately 1,200 fold to 300 fold lower than the level of the corresponding transcripts in their spleens, respectively. We also detected mRNA in both spleens and corneas of SCID mice, which are known to lack functional $CD4^+$ and $CD8^+$ T cells as determined by

Table 2. Number of $CD4^+$ and $CD8^+$ T cells in mouse cornea

		Cells/total corneas		Cells/ individual cornea		
Mouse strain	Age	CD4+	CD8+	CD4+	CD8+	Total
ICR	19 month	306 (n=44)	495 (n=44)	7.0	11	25000
ICR	4 weeks	209 (n=66)	54 (n=66)	3.2	0.8	7575
BALB/c	8 weeks	802 (n=50)	109 (n=50)	16	2.2	16666
C57BL/6	8 weeks	164 (n=80)	119 (n=80)	2.0	1.5	13750
SCID	8 weeks	ND (n=20)	ND (n=20)	ND	ND	8750

Corneas from each group of mice were harvested and combined as described in Methods. Single cell suspensions of corneas were reacted with mAbs to 7ADD/CD4/CD8 and the number of $CD4^+$, or $CD8^+$ cells and $7ADD^-$ cells were sorted using a MoFlo (Dako). In the table, "ND" indicates not determined and n=the number of total mice corneas used in each group.

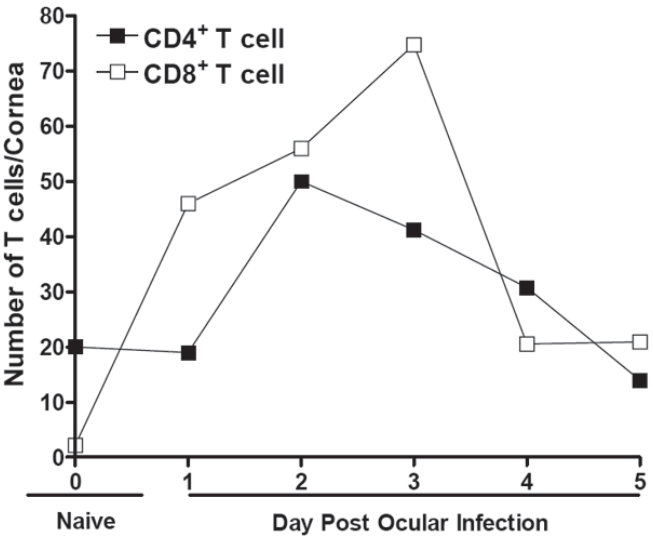

Figure 6. Cell sorting of $CD4^+$ and $CD8^+$ T cells in corneas of infected mice. BALB/c mice were ocularly infected with $2x10^5$ PFU/eye of HSV-1 strain McKrae as described in the legend to Figure 5. Corneas from 10 mice per time point were isolated without contamination from other parts of the eye as described in Methods. Ten naive mice were also used as control. Single cell suspensions of corneas were reacted with mAbs to 7-ADD/CD4/CD8, and the number of $CD4^+$ or $CD8^+$ T cells and $7\text{-}ADD^-$ T cells were sorted using a MoFlo (Dako). Data are presented as the number of $CD4^+7\text{-}ADD^-$ or $CD8^+7\text{-}ADD^-$ cells per cornea.

serological or functional assays. Our findings with regard to the detection of mRNA in spleen and corneas of SCID mice was not unexpected since similar results have been reported previously, showing that SCID mice are "leaky" and generate a few clones of functional T cells [22-27]. As expected the levels of these transcripts in SCID mice were significantly lower than the levels of the corresponding transcripts in BALB/c and C57BL/6 mice. However, we did not detect any $CD4^+$, $CD8^+$, or $CD3^+$ T cells in corneas of SCID mice by immunostaining. The number of CD4 and CD8 transcripts per μg of corneal RNA was similar between BALB/c and C57BL/6 mice. Likewise, the number of $CD8^+$ T cells per cornea of both BALB/c and C57BL/6 mice was the same. At the same time, the number of $CD4^+$ T cells per cornea of BALB/c mice was higher than the number of $CD4^+$ T cells per cornea of C57BL/6 mice despite a similar number of CD4 transcripts. This discrepancy between the number of CD4 transcripts versus the number of $CD4^+$ T cells in corneas of BALB/c mice compared with C57BL/6 mice could be due to presence of higher amounts of total RNA isolated from corneas of BALB/c mice.

Collectively, these data demonstrate for the first time that the central cornea of naive mice contain both $CD4^+CD3^+$ and $CD8^+CD3^+$ T cells. Previously, T cells were only detected in the cornea after traumatic insult or injury. Based on the absence of detectable levels of T cells in the normal cornea, it was concluded that the cornea is a simple collagenous tissue that is dependent on the migration of T cells from the host immune system for appropriate immune responses to stress. In particular, the presence of T cells in the cornea before infection may be of importance in our understanding and development of treatment strategies for diseases of the cornea that are associated with the T-cell response to infectious agents. In this regard, it was recently shown that adding corneal-derived fibroblasts infected with HSV-1 to HSV-1-infected splenocytes abrogated the cytotoxic response while enhancing IFN-γ production by HSV-specific cytotoxic T lymphocytes (CTL) [28]. This suppressive effect of corneal-derived fibroblasts on the CTL activity of cells isolated from the same mouse spleen could be due to the presence of $CD4^+$ and/or $CD8^+$ T cells in the isolated corneal cell population.

Finally, with regard to the presence of CD4 or CD8 transcripts and $CD4^+$ or $CD8^+$ T cells in corneas of HSV-1 infected control mice, we did not detect any significant differences between BALB/c mice that are susceptible to herpes stromal keratitis (HSK) compared with C57BL/6 mice, which are highly resistant to HSK [29,30]. Our results are in contrast to a previously published study that suggested $CD4^+$ T cells play an important role in induction of the disease in mice susceptible to HSV-1 [31,32]. This higher susceptibility of BALB/c mice could be due to an increase in $CD4^+$ T cell infiltrates into the corneas compared with C57BL/6 mice. However, our results showed a decline in the number of both $CD4^+$ and $CD8^+$ T cells in the corneas of BALB/c mice from day one to day five post-ocular infection. We also have shown that the number of $CD4^+$ T cells significantly declines after day seven post-infection in both immunized and mock immunized mice [10,11]. Although the number of $CD4^+$ T cells in naive mice was similar to that of infected mice on day five post-infection, there was an approximately 10 fold increase in the number of CD8+ T cells in naive and infected mice. Consistent with this observation, we recently have shown that $CD8^+$ T cells rather than $CD4^+$ T cells are involved in exacerbation of corneal scarring [33].

Thus, the observations described herein may lead to a paradigm shift in our understanding of corneal immunity. It may be necessary to move away from the concept of the cornea as a passive bystander to a model that incorporates its role as an active participant in orchestrating its own immune system in response to foreign or autoantigens [10,11]. The knowledge of the presence of resident corneal T cells despite their possible rarity may alter our overall perception of the various models of corneal diseases and protection.

ACKNOWLEDGEMENTS

This work was supported by NIH grant EY14966 and the Skirball Program in Molecular Ophthalmology to H.G.

REFERENCES

1. Streilein JW. Ocular immune privilege: the eye takes a dim but practical view of immunity and inflammation. J Leukoc Biol 2003; 74:179-85.
2. Green DR, Ferguson TA. The role of Fas ligand in immune privilege. Nat Rev Mol Cell Biol 2001; 2:917-24.
3. Cursiefen C, Chen L, Dana MR, Streilein JW. Corneal lymphangiogenesis: evidence, mechanisms, and implications for corneal transplant immunology. Cornea 2003; 22:273-81.
4. Planck SR, Rich LF, Ansel JC, Huang XN, Rosenbaum JT. Trauma and alkali burns induce distinct patterns of cytokine gene expression in the rat cornea. Ocul Immunol Inflamm 1997; 5:95-100.
5. Rosenbaum JT, Planck ST, Huang XN, Rich L, Ansel JC. Detection of mRNA for the cytokines, interleukin-1 alpha and interleukin-8, in corneas from patients with pseudophakic bullous keratopathy. Invest Ophthalmol Vis Sci 1995; 36:2151-5.
6. Kuffova L, Holan V, Lumsden L, Forrester JV, Filipec M. Cell subpopulations in failed human corneal grafts. Br J Ophthalmol 1999; 83:1364-9.
7. Williams KA, Standfield SD, Mills RA, Takano T, Larkin DF, Krishnan R, Russ GR, Coster DJ. A new model of orthotopic penetrating corneal transplantation in the sheep: graft survival, phenotypes of graft-infiltrating cells and local cytokine production. Aust N Z J Ophthalmol 1999; 27:127-35.
8. Hazlett LD, McClellan SA, Rudner XL, Barrett RP. The role of Langerhans cells in Pseudomonas aeruginosa infection. Invest Ophthalmol Vis Sci 2002; 43:189-97.
9. Hazlett LD, McClellan S, Kwon B, Barrett R. Increased severity of Pseudomonas aeruginosa corneal infection in strains of mice designated as Th1 versus Th2 responsive. Invest Ophthalmol Vis Sci 2000; 41:805-10.
10. Ghiasi H, Wechsler SL, Kaiwar R, Nesburn AB, Hofman FM. Local expression of tumor necrosis factor alpha and interleukin-2 correlates with protection against corneal scarring after ocular challenge of vaccinated mice with herpes simplex virus type 1. J Virol 1995; 69:334-40.
11. Ghiasi H, Wechsler SL, Cai S, Nesburn AB, Hofman FM. The role of neutralizing antibody and T-helper subtypes in protec-

tion and pathogenesis of vaccinated mice following ocular HSV-1 challenge. Immunology 1998; 95:352-9.
12. Bendelac A. Mouse NK1+ T cells. Curr Opin Immunol 1995; 7:367-74.
13. Norian LA, Allen PM. No intrinsic deficiencies in CD8+ T cell-mediated antitumor immunity with aging. J Immunol 2004; 173:835-44.
14. Takahashi K, Nakata M, Tanaka T, Adachi H, Nakauchi H, Yagita H, Okumura K. CD4 and CD8 regulate interleukin 2 responses of T cells. Proc Natl Acad Sci U S A 1992; 89:5557-61.
15. Frei K, Eugster HP, Bopst M, Constantinescu CS, Lavi E, Fontana A. Tumor necrosis factor alpha and lymphotoxin alpha are not required for induction of acute experimental autoimmune encephalomyelitis. J Exp Med 1997; 185:2177-82.
16. Iwamoto T, Smelser GK. Electron microscope studies on the mast cells and blood and lymphatic capillaries of the human corneal limbus. Invest Ophthalmol 1965; 4:815-34.
17. Streilein JW, Toews GB, Bergstresser PR. Corneal allografts fail to express Ia antigens. Nature 1979; 282:326-7.
18. Gebhardt BM. The role of class II antigen-expressing cells in corneal allograft immunity. Invest Ophthalmol Vis Sci 1990; 31:2254-60.
19. Hamrah P, Liu Y, Zhang Q, Dana MR. The corneal stroma is endowed with a significant number of resident dendritic cells. Invest Ophthalmol Vis Sci 2003; 44:581-9.
20. Brissette-Storkus CS, Reynolds SM, Lepisto AJ, Hendricks RL. Identification of a novel macrophage population in the normal mouse corneal stroma. Invest Ophthalmol Vis Sci 2002; 43:2264-71.
21. Ferguson TA, Griffith TS. A vision of cell death: Fas ligand and immune privilege 10 years later. Immunol Rev 2006; 213:228-38.
22. Bosma GC, Fried M, Custer RP, Carroll A, Gibson DM, Bosma MJ. Evidence of functional lymphocytes in some (leaky) scid mice. J Exp Med 1988; 167:1016-33.
23. Carroll AM, Hardy RR, Petrini J, Bosma MJ. T cell leakiness in scid mice. Curr Top Microbiol Immunol 1989; 152:117-23.
24. Bosma MJ, Carroll AM. The SCID mouse mutant: definition, characterization, and potential uses. Annu Rev Immunol 1991; 9:323-50.
25. Carroll AM, Bosma MJ. Detection and characterization of functional T cells in mice with severe combined immune deficiency. Eur J Immunol 1988; 18:1965-71.
26. Schuler W, Schuler A, Lennon GG, Bosma GC, Bosma MJ. Transcription of unrearranged antigen receptor genes in scid mice. EMBO J 1988; 7:2019-24.
27. Shores EW, Sharrow SO, Uppenkamp I, Singer A. T cell receptor-negative thymocytes from SCID mice can be induced to enter the CD4/CD8 differentiation pathway. Eur J Immunol 1990; 20:69-77.
28. Knickelbein JE, Divito S, Hendricks RL. Modulation of CD8+ CTL effector function by fibroblasts derived from the immunoprivileged cornea. Invest Ophthalmol Vis Sci 2007; 48:2194-202.
29. Ghiasi H, Cai S, Perng GC, Nesburn AB, Wechsler SL. Both CD4+ and CD8+ T cells are involved in protection against HSV-1 induced corneal scarring. Br J Ophthalmol 2000; 84:408-12.
30. Ghiasi H, Cai S, Perng GC, Nesburn AB, Wechsler SL. The role of natural killer cells in protection of mice against death and corneal scarring following ocular HSV-1 infection. Antiviral Res 2000; 45:33-45.
31. Newell CK, Martin S, Sendele D, Mercadal CM, Rouse BT. Herpes simplex virus-induced stromal keratitis: role of T-lymphocyte subsets in immunopathology. J Virol 1989; 63:769-75.
32. Babu JS, Thomas J, Kanangat S, Morrison LA, Knipe DM, Rouse BT. Viral replication is required for induction of ocular immunopathology by herpes simplex virus. J Virol 1996; 70:101-7.
33. Osorio Y, Cai S, Hofman FM, Brown DJ, Ghiasi H. Involvement of CD8+ T-cells in exacerbation of corneal scarring in mice. Curr Eye Res 2004; 29:145-51.

The print version of this article was created on 28 Sep 2007. This reflects all typographical corrections and errata to the article through that date. Details of any changes may be found in the online version of the article.